

University of Cincinnati ILL

ILLiad TN: 73442



DATE: 6/28/2005 04:31:36 PM

Borrower: MUB

Call #: TK7871.85 .A3482 2002

Lending String: *CIN,CIN,OKU,SEA

Location: ENGR Stacks AVAILABLE

Patron: DEPT; STATUS: Gobbert, Matthias

Journal Title: Advanced Metallization Conference 2002 (AMC 2002) ; proceedings of the conference held October 1-3, 2002, in San Diego, California, U.S.A., and Octobe

OCLC: 55046503

Volume: Issue:

Month/Year: 2002**Pages:** 709-715 copy of chapter

Article Author: Advanced Metallization Conference (2002 ; San Diego, Calif. and Tokyo, Japan)

Article Title: Vinay Prasad, Matthias K. Gobbert, Max Bloomfield, and Timothy S. Cale; Improving Pulse Protocols in Atomic Layer Deposition

Imprint: Warrendale, Pa. ; Materials Research Soc

ILL Number: 10389867



ARIEL

Charge

Maxcost: \$20IFM

Shipping Address:

Albin O. Kuhn Library & Gallery
University of Maryland, Baltimore County
1000 Hilltop Circle
Baltimore, MD 21250

Fax:

Ariel: 130.85.150.114

IMPROVING PULSE PROTOCOLS IN ATOMIC LAYER DEPOSITION

¹Vinay Prasad, ²Matthias K. Gobbert, ¹Max Bloomfield, and ¹Timothy S. Cale

¹Focus Center - New York, Rensselaer: Interconnections for Gigascale Integration
Rensselaer Polytechnic Institute, CII 6015, 110 8th Street, Troy, NY 12180-3590

²Department of Mathematics and Statistics, University of Maryland, Baltimore County,
1000 Hilltop Circle, Baltimore, MD 21250

ABSTRACT

We show how to use limited rate data from studies of atomic layer deposition (ALD), as commonly found in the literature, to develop or improve pulse protocols. One major point is that purge times should be minimized not only because of the time involved, but also because of the possibility of desorption of adsorbed reactants. To quantify the effects of pulse protocols, we estimate parameters in a simple surface chemistry model. We use the model to predict surface coverages and monolayers deposited over ALD cycles. We use such results, even with large uncertainties due to the limited data available, to show how pulse protocols can be developed for four ALD processes; 1) tungsten nitride ALD using WF_6 and ammonia, 2) plasma-enhanced ALD (PEALD) of Ti using $TiCl_4$ and atomic hydrogen, 3) PEALD TaN using tertbutylimidotris(diethylamido)tantalum (TBTDET) and a hydrogen plasma, and 4) ALD TaN using TBTDET and ammonia. The latter two are considered together, and the suggested protocols are compared with experimental data, and suggested pulse protocols significantly increase the deposition rate, assuming that the flows and power can be switched at the proposed speeds. After suggesting a pulse protocol for WN ALD, we show that desorption doesn't seem to be an issue in the Ti PEALD process studied. Thus, rapid purges only decrease cycle time, but do not affect monolayers per cycle.

INTRODUCTION

Atomic layer deposition (ALD) has attracted attention because of the possibility of self-limiting, monolayer-by-monolayer depositions [1-4]. Much of the relevant literature on feature scale modeling of ALD consists of descriptions of surface mechanisms without a detailed model for gas phase transport [5, 6]. In this paper, we show that this approach is reasonable from a transport point of view. We focus on the feature scale and idealize changes at the reactor scale, *i.e.*, changes in flow and concentrations are assumed to occur such that changes directly over the feature can be considered to occur as step functions. Thus, all fluxes from the reactor volume to the feature mouth are constant in time, except for step changes at the start and stop of a pulse.

The dominant approach to deterministic feature scale transport and reaction analyses was developed to model topography evolution during conventional steady-state deposition and etch processes. These models are pseudo-steady, *i.e.*, the local surface reaction rates are computed assuming fluxes are constant in time [7], determining the growth rates based in a consistent manner, and then evolving the surface in small time increments. EVOLVE [7, 8] offers a comprehensive framework for feature scale topography simulation during such pseudo-steady deposition and etch process simulation. Due to the periodic pulsing of reactants and purge gases, a comprehensive model for ALD should start with the transient nature of the process, and include models for gas phase transport and surface chemistry. We have developed a transient, Boltzmann equation based transport and reaction model for ALD [9-12]. The transport model has no adjustable parameters, though models for species re-emission from surfaces are needed. Heterogeneous reaction mechanisms are used to express adsorption, desorption, and surface reaction. Results for the adsorption and post-adsorption purge steps, and for the reaction and post-reaction purge steps are presented in Refs. 10 and 11. While desorption of reactants may not be a concern in some ALD processes, in general it should be considered possible in the absence of clear data that support irreversible surface reactions.

The goal of this paper is to describe how incomplete data on reaction rates in ALD, as typically reported in the literature, can be used to improve pulse protocols (pulse and purge times) for four ALD systems. Two of the systems involve plasma-enhanced ALD (PEALD), which has recently been investigated [13-15] as a possible method to increase surface reaction rates and improve deposited film

properties. We fit kinetic parameters in our surface reaction models to interpret experimental data on the dependence of deposition rates on reactant pulse times for TaN PEALD using tertbutylimidotris(diethylamido)tantalum (TBTDET) and hydrogen radicals as described in Ref. 15, and for Ti PEALD using TiCl_4 and atomic hydrogen as described in Ref. 16. We also fit models to interpret experimental data on tungsten nitride ALD using WF_6 and ammonia as described in Ref. 17 and TaN ALD from TBTDT and ammonia. We start by briefly reviewing the transport and reaction models used, as well as some overall results of the BTE solutions.

MODEL

Feature Scale Transport Model

For this paper, we consider the two-dimensional cross-section of a feature with aspect ratio $A = 4$, as shown in Fig. 1. The width of the feature mouth is taken as $L = 0.25 \mu\text{m}$. The domain consists of the interior of the feature and a small area of gas inside the Knudsen layer above the wafer surface. The transport of the inert carrier gas and the reactive species through the domain is described by a set of Boltzmann transport equations (BTEs). Assuming that the reactive species are at least an order of magnitude less concentrated than the carrier gas, it is possible to decouple the BTE for the inert carrier, and to solve a system of BTEs for the reactive species [10, 11].

We assume that the inflow conditions at the interface to the bulk of the reactor chamber are specified and homogeneous in space and time. For neutral species, we use a Maxwellian distribution. At the sides of the domain above the wafer surface, we use specular reflection to simulate periodic features. At the wafer surface, we model the emission of gaseous molecules into the computational domain as diffusive emission by prescribing a Maxwellian velocity distribution for neutral species: In the absence of reactions, the inflowing density distribution is modeled as being proportional to the flux to the surface for each species η_i ; if reactions are present, the rates R_i of the surface reactions increase or decrease the inflowing density distribution, depending upon whether the species is consumed or generated by the surface reactions.

The BTEs are nondimensionalized using reference quantities for concentration and speed of the reactant species [10, 11]. The reference concentration and speed are chosen to be the corresponding quantities for A, the "first" reactive species in each system. For each system, the precursor (organometallic or halide) is designated to be the first reactive species.

Surface Reaction Model

The surface chemistry model accounts for reaction of precursor with the co-reactant. For the two cases with plasma-enhanced ALD, we designate hydrogen radicals to be the second reactive species (B). In the case of tungsten nitride ALD, ammonia is the second species. Our surface reaction model consists of reversible adsorption of A on a single site, and irreversible reaction of B with the adsorbed A:



where A_v is adsorbed A, v stands for a surface site available for adsorption, and $(*)$ is the non-adsorbing gaseous product. Surface sites for adsorption are produced by the reaction of B with adsorbed A.

If the fraction of surface sites occupied by molecules of species A is denoted by ϑ_A , the reaction rates, made dimensionless by dividing them by the flux of species A to the wafer well away from any feature [10, 11], can be written as

$$\begin{aligned} R_1 &= \gamma_1^f (1 - \vartheta_A) \eta_1 - \gamma_1^b \vartheta_A \\ R_2 &= \gamma_2^f \vartheta_A \eta_2 \end{aligned} \quad (2)$$

where η_i denotes the (dimensionless) flux of species i to the surface, and γ_1^f , γ_1^b , and γ_2^f are (dimensionless) rate parameters associated with adsorption, desorption, and reaction of A with B,

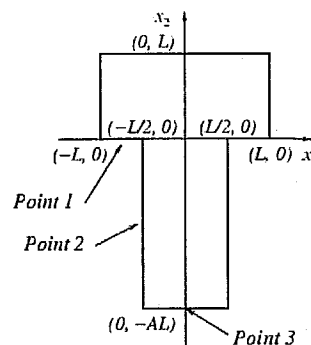


Figure 1. Schematic of a two-dimensional domain defining length L and aspect ratio A .

models to interpret experimental data on the growth of TaN PEALD using oxygen radicals as described in Ref. 15, and in Ref. 16. We also fit models to interpret ammonia as described in Ref. 17 and TaN using the transport and reaction models used,

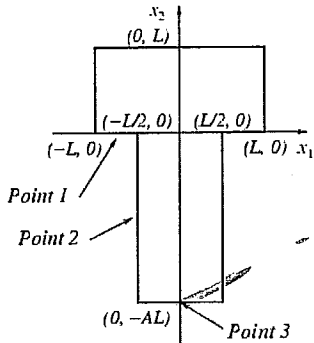


Figure 1. Schematic of a two-dimensional domain defining length L and aspect ratio A .

wafer surface, we use specular reflection to the emission of gaseous molecules into the Maxwellian velocity distribution for neutral adsorption is modeled as being proportional to the rates R_i of the surface reactions depending upon whether the species is consumed

properties for concentration and speed of the species. For each system, the precursor species.

for adsorption, and (*) is the non-adsorbing reaction of B with adsorbed A. Species A is denoted by \mathcal{G}_A , the reaction rates, A to the wafer well away from any feature

$$(1)$$

for adsorption, and (*) is the non-adsorbing reaction of B with adsorbed A. Species A is denoted by \mathcal{G}_A , the reaction rates, A to the wafer well away from any feature

$$(2)$$

to the surface, and γ^f , γ^b , and γ^s are desorption, and reaction of A with B,

respectively. The dimensionless fluxes and reaction rates can be re-dimensionalized by multiplying them by the flux of species A. The dimensionless rate parameters can be re-dimensionalized using the flux of species A and the total number of sites available for adsorption per unit area.

The evolution of \mathcal{G}_A at every point of the wafer surface is given by

$$\frac{d\mathcal{G}_A(t)}{dt} = \alpha_p (R_1(t) - R_2(t)), \quad \mathcal{G}_A(0) = \mathcal{G}_A^{ini} \quad (3)$$

where the initial coverage \mathcal{G}_A^{ini} is known and α_p is a constant prefactor arising from the non-dimensionalization procedure. In general, this differential equation cannot be solved in closed form, because its coefficients depend on the fluxes η . However, if we can justify the assumption that the fluxes are constant in time, an analytic solution for the fractional coverage \mathcal{G}_A can be obtained (see [10, 11]).

RESULTS

We present the results of three case studies, tungsten nitride ALD using WF_6 and ammonia, Ti ALD using $TiCl_4$ and atomic hydrogen, and TaN ALD using TBTDDET and hydrogen plasma. For all these cases, simulation results show that transport is fast compared to reaction. Figures 2a and 2b show representative distributions of the dimensionless number density of A, the first reactive species, throughout the gas domain during the adsorption step at $t = 5$ ns and 40 ns. After 5 ns, the gas has not filled the interior of the feature yet; after 40 ns the feature has filled completely with gas. This demonstrates that the transport is much faster than the typical duration of the adsorption step (which may be of the order of a second or longer). Similarly, the gas is transported out of the feature domain over a time scale much shorter than the typical duration of the pulse during the post-adsorption purge. Figure 3 shows the flux to the surface of species A vs. time at the three observation points (see Fig. 1); Fig. 3a for the adsorption step and Fig. 3b for the post-adsorption purge step. Observe that in both processing steps, the flux tends to equilibrium more slowly than the gas fill of the domain, but significantly faster than typical pulse times for adsorption and post-adsorption purge. Additionally, the fluxes tend to a spatially uniform constant value. Similar results indicating fast transport compared to reaction are obtained for the reaction and post-reaction purge steps. For similar and more detailed results on each step of the ALD cycle, see Refs. 10 and 11.

Tungsten Nitride ALD

The experimental data we calibrate our model against in this study were obtained from Klaus *et al.* [17], who studied tungsten nitride ALD using WF_6 and ammonia. The data were obtained at a temperature of 600 K, with a WF_6 partial pressure between 1-10 mTorr during its pulse and NH_3 partial pressure of 1-10mTorr during its pulse. The N_2 purges separating the WF_6 and NH_3 pulses were 1-3 minutes long. For the simulations, we used conditions of 1 mTorr of WF_6 during its

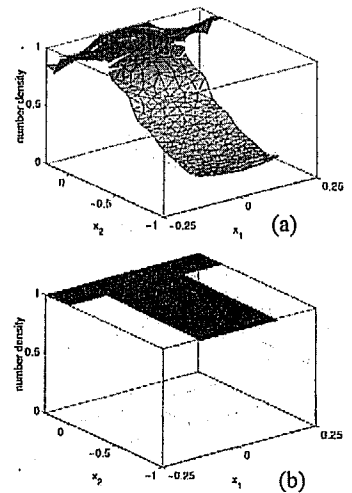


Figure 2. Adsorption step, assuming a step change in flux from the reactor volume at $t=0$; reasonable features fill in less than 100 ns. The dimensionless number density of species A for a trench with aspect ratio 4 at (a) 5.0 ns, (b) 40.0 ns. Note that the scales on the x_1 and x_2 axes are different.

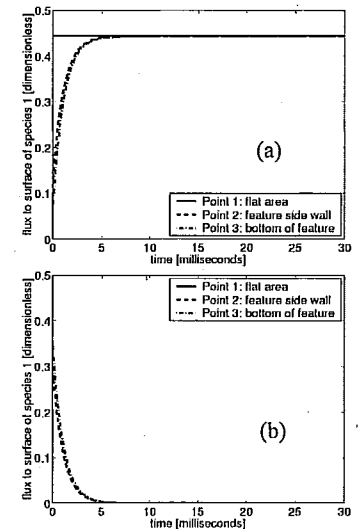


Figure 3. Dimensionless flux of species A to the surface vs. time during (a) adsorption, (b) post-adsorption purge.

pulse and 1 mTorr of NH_3 during its pulse, and we assume that the N_2 purges are 2 minutes long. Klaus *et al.* state that the reaction of WF_6 and ammonia occurs as a set of two half-reactions, with the ammonia serving to remove the fluorine terminated group from the adsorbed species. We use the surface chemistry model described above to approximate this chemistry. We adjust kinetic parameters in our surface reaction model to provide the best fit of model predictions to the experimental data. Figure 4 shows a comparison of model predicted monolayers per cycle as a function of NH_3 and WF_6 pulse times with experimental data from Ref. 17. The values obtained for the kinetic parameters are $\gamma_1^f = 1.5 \times 10^{-2}$ for the adsorption rate constant, $\gamma_1^b = 2.5 \times 10^{-5}$ for the desorption rate constant, and $\gamma_2^f = 2.8 \times 10^{-2}$ for the reaction rate constant. Fairly good agreement is obtained between the model predictions and experimental data. Using these kinetic parameters, we predict surface coverage and monolayers deposited per cycle for a suggested protocol that is based upon the estimated rate parameters; the results are presented in Fig. 5. Based on the model predictions, a pulse protocol with WF_6 pulses of approximately 4.5 seconds, NH_3 pulses of 6 seconds, and short purges (1 second long) provides good deposition thickness per ALD cycle. Of course, different assumed values of the fluxes (partial pressures) would yield different parameters and different pulse protocol details. A different chemistry model, with perhaps more parameters, would also yield different results.

Ti PEALD

The experimental data we calibrate our model against in this study were obtained from Kim and Rosnagel [16], who studied plasma-enhanced ALD of Ti using TiCl_4 and atomic hydrogen at room temperature. TiCl_4 exposures of 10^4 Langmuir (10^{-6} torr-sec) were used for most experiments in Ref. 16. Details on purge times are not explicitly given in Ref. 16. Similarly, atomic hydrogen fluxes were not reported. We assume conditions of 10 mTorr of TiCl_4 during its pulse, and we assume that the purges are short, approximately 1 second long. We use the surface chemistry model described in an earlier section to approximate the surface chemistry. We adjust kinetic parameters in our surface reaction model to provide the best fit of model predictions to the experimental data. Figure 6 shows a comparison of model predicted monolayers per cycle as a function of hydrogen exposure time with experimental data from Ref. 16. The values obtained for the kinetic parameters are $\gamma_1^f = 5.0 \times 10^{-2}$ for the adsorption rate constant, $\gamma_1^b = 4.1 \times 10^{-6}$ for the desorption rate constant, and $\eta_2 \gamma_2^f = 1.73 \times 10^{-6}$ for the product of the reaction rate constant and the dimensionless steady state flux of atomic hydrogen. Good agreement is obtained between the model predictions and experimental data. Note that our kinetic model differs from that of Kim and Rosnagel [16] in that we consider the possibility of desorption. The low value of desorption rate constant relative to the adsorption rate constant indicates that

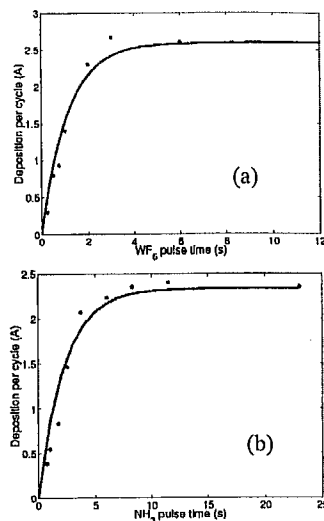


Figure 4. Comparison of predicted deposition rate with experimental data taken from [17] for varying (a) WF_6 pulse times and (b) NH_3 pulse times.

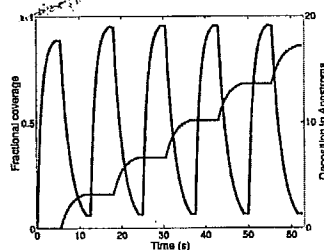


Figure 5: Predicted surface coverage and monolayers deposited for five WN ALD cycles using suggested pulse protocol.

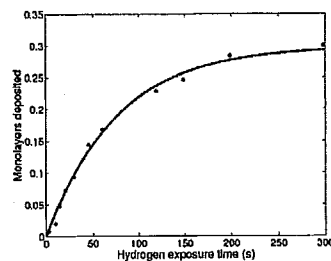


Figure 6: Comparison of predicted Ti monolayers deposited during Ti PEALD as a function of hydrogen exposure time with experimental data from [16].

desorption may not be a significant factor in our kinetic model. The relatively large fraction of desorption noted that the experimental data shows that the rate would suggest a pulse

TaN PEALD and

The experimental data from [15], who conducted enhanced ALD. The TaN layer is long, and the NH_3 pulse is long.

During the reaction, TaN ions are highly mobile and lead to very large deposition rates due to the feature if the ions are not removed by the films grown by PEALD. Within features, the ion fluxes do not decrease, leading to enhanced ALD and PEALD reaction affecting the

Given the fact that the experimental data from Refs. 10 and 11 show a function of pulse species to match the ALD and PEALD, respectively, radical terminated adsorption and desorption kinetic parameters

rate constant, γ_2^f for PEALD, and $\gamma_1^f = 6.0 \times 10^{-5}$ for the reaction rate constant. The model predictions using the experimental data achieved between the experimental data and the reaction between the ALD and PEALD than for reaction between hydrogen radicals. Also, the adsorption rate when hydrogen radicals with the conclusion rate results in a factor of 10 per cycle with respect to the

Based on our kinetic model, the monolayers deposited per cycle used by PEALD is observed to be drops from approximately 0.3 monolayers per cycle to approximately 0.1 monolayers per cycle adsorbed TBDET

desorption may not be a significant factor in this process. The experimental data and the fitted parameter values in our kinetic model suggest that a fairly long reaction step is required to obtain deposition of a relatively large fraction of a monolayer in one cycle at the specified experimental conditions. It should be noted that the experimental data in Fig. 6 were taken with an aperture to reduce the hydrogen atom flux, so that the rate would be slow enough to follow. Because desorption doesn't seem to be an issue, we do not suggest a pulse protocol for this ALD system.

TaN PEALD and ALD

The experimental data we calibrate our model against in this case study were obtained from Park *et al.* [15], who conducted a comparison of ALD using NH_3 as the reducing agent, and (hydrogen) plasma enhanced ALD. The TBTDET pulse time was varied between 1 s and 6 s. All the purge times were 15 s long, and the NH_3 and hydrogen plasma pulses were 10 s long in ALD and PEALD, respectively.

During the reaction step, we seek to investigate the effect ions may have on the deposition rate of TaN. Ions are highly directed species, and the source flux distribution for ions is very narrow. This would lead to very large fluxes of ions at middle of the bottom of the feature as compared to the sidewalls. If the deposition rate due to ions depends on the ion flux, then we would see nonconformal deposition inside the feature if the ions contributed significantly to the deposition rate. However, Park *et al.* [15] state that the films grown by PEALD show excellent step coverage, and there is no variation depending on position within features, i.e., the growth is the same at the bottom and sidewalls. This leads us to conclude that the ion fluxes do not directly affect the deposition rates. Since we are interested in predicting deposition rates in ALD and PEALD, we focus on the reaction between hydrogen radicals and TBTDET as being the sole reaction affecting the fraction of monolayers deposited per PEALD cycle.

Given the fact that transport is fast compared to reaction, we use the analytical solution developed in Refs. 10 and 11 to track monolayer coverage and deposition rates over many ALD cycles and as a function of pulse times. We fit the kinetic parameters in our model for surface coverage of adsorbed species to match the dependence of monolayers deposited per cycle on TBTDET pulse time for PEALD and ALD, respectively. Since Park *et al.* [15] postulate that the adsorption rate of TBTDET on a hydrogen radical terminated film is different than its adsorption rate on a NH_3 terminated film, we do not force the adsorption and desorption rate parameters to be the same values in both cases. The values obtained for the kinetic parameters are $\gamma_1^f = 6.0 \times 10^{-3}$ for the adsorption rate constant, $\gamma_1^b = 1.2 \times 10^{-4}$ for the desorption

rate constant, $\gamma_2^f = 5.1 \times 10^{-1}$ for the reaction rate constant in PEALD, and $\gamma_1^f = 3.4 \times 10^{-3}$ for the adsorption rate constant, $\gamma_1^b = 6.0 \times 10^{-5}$ for the desorption rate constant, $\gamma_2^f = 2.9 \times 10^{-1}$ for the reaction rate constant in ALD using NH_3 . The model predictions using these fitted parameters are plotted against the experimental data from [15] in Fig. 7. Good agreement is achieved between the fitted model predictions and experimental data. The reaction rate parameter is higher for reaction between adsorbed TBTDET and hydrogen radicals than for reaction between TBTDET and NH_3 , indicating that hydrogen radicals are more reactive than NH_3 in this situation. Also, the adsorption rate parameter for TBTDET is higher when hydrogen radicals are present, which is in agreement with the conclusions of Park *et al.* [15]. The higher adsorption rate results in a faster saturation time of monolayers deposited per cycle with respect to TBTDET pulse time.

Based on our fits of the kinetic parameters of the chemistry models, we predict fractional coverage and monolayers deposited over 5 PEALD cycles. Figure 8a shows fractional coverage and monolayers deposited for the pulse cycle used by Park *et al.*; significant loss of coverage due to desorption is observed. The fractional coverage of TBTDET drops from approximately 0.9 to 0.35 during the post-adsorption purge in each ALD cycle. Additionally, the adsorbed TBTDET is consumed by reaction during the first 1 s

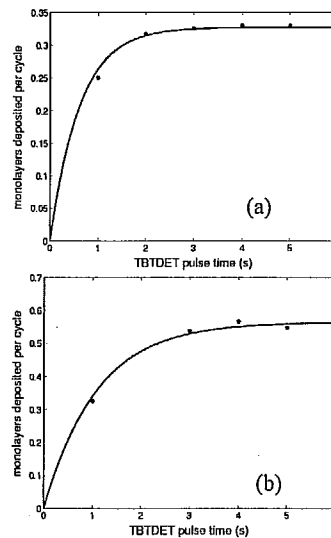


Figure 7. Comparison of model predicted monolayers deposited per cycle against experimental data from [15] for (a) PEALD, (b) ALD.

of the reaction step; there is no deposition during the rest of the reaction step. In the post-reaction purge, the reactants are purged out of the feature domain on the order of milliseconds. This indicates that the purges and the reaction step can be shortened to increase monolayer deposition per unit time. Shortening the post-adsorption purge reduces the loss of adsorbed TBTDET due to desorption, and keeps surface coverage high at the start of the reaction step. Reducing the durations of the reaction step and the post-reaction purge does not affect the monolayer deposition, but results in shortening the duration of the ALD cycle. Figure 8b shows predictions of fractional coverage and monolayers deposited when the purge times are shortened to 0.5 s, and the reaction step is shortened to 1 s. The duration of the PEALD cycle is considerably shortened, and approximately 0.9 monolayers are deposited per cycle. The contribution of desorption to consumption of adsorbed TBTDET is significantly reduced, and almost all the adsorbed TBTDET is consumed by reaction.

In Fig. 9, we show predictions of fractional coverage and monolayers deposited over 5 cycles for TaN ALD using NH_3 as the co-reactant. Figure 9a shows fractional coverage and monolayers deposited for the pulse cycle used by Park *et al.*; significant loss of coverage due to desorption is observed, as was the case with PEALD. Significant desorption during the post-adsorption purge is observed here in Fig. 9b, the fractional coverage drops from approximately 0.9 to 0.55. As in the case of TaN PEALD, the reaction and post-reaction purge steps are too long, and can be shortened significantly. Figure 9b shows predictions of fractional coverage and monolayers deposited when the purge times are shortened to 0.5 s, and the reaction step is shortened to 1 s. Approximately 0.9 monolayers are deposited per cycle, and one cycle is 6 s long as opposed to 44 s for the original pulse protocol.

CONCLUSIONS

We use results from studies with a transient, Boltzmann equation based transport and reaction model, and a simple chemistry model to suggest how limited data might be used to develop ALD pulse protocols. We use the calibrated chemistry models to predict surface coverage and monolayers deposited over several ALD cycles, and to develop pulse protocols. We chose four processes from the literature [15-17]. We suggest a pulse protocol for WN ALD that is on the order of 10 seconds per cycle. For Ti PEALD, desorption doesn't seem to be an issue, so long purge times only affect ALD cycle time and not the monolayers per cycle. For TaN PEALD, we conclude that the monolayers per cycle can be increased relative to the experimental data by shortening the post-adsorption purge time; this decreases reactant desorption. The overall growth rate can be increased by decreasing co-reactant and post-reaction purge pulse times; they are too long. For TaN PEALD, in addition to the fast switching between process streams required to keep the purge times as low as 0.5 s, the pulsing of the plasma also needs to be achieved in 1 s.

We have not made any attempt to study the constraints placed on any of the experimental systems by process limitations. We do not know if the durations specified for the reaction step and the purges could

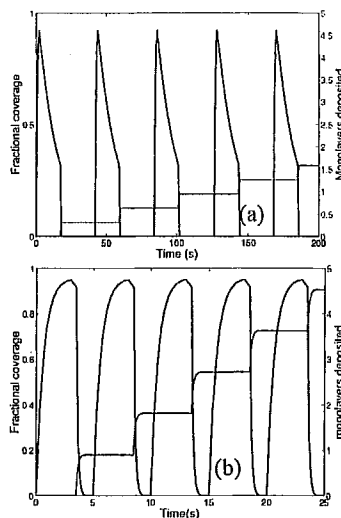


Figure 8. Fractional coverage and monolayers deposited during PEALD for (a) pulse cycle of Park *et al.* [15], and (b) shortened pulse cycle.

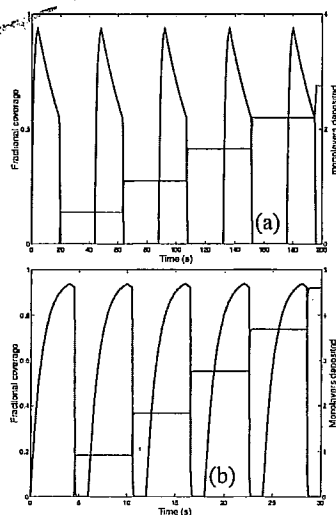


Figure 9. Fractional coverage and monolayers deposited during ALD using NH_3 for (a) pulse cycle of Park *et al.* [15], and (b) shortened pulse cycle.

be achieved Fig. 5, Fig. fashion.

The representation as well as the model we use chemistry model also provide goal of the if more rele

ACKNOWLEDGMENT

The RPI aut Center.

REFERENCES

- [1] M. Rit
- [2] M. Le
- [3] T. Sun
- [4] H. Stin
- [5] J.-W. .
- [6] H.-S. .
- [7] T. S. C
- [8] EVOL
- [9] M. K. 1999. *Depos Societ*
- [10] M. K.
- [11] M. K.
- [12] M. K.
- [13] S. M. .
- [14] J.-S. P
- [15] J.-S. P
- [16] H. Kir Ti Ato
- [17] J. W. using

be achieved using today's processing equipment. Therefore, our recommended pulse sequences shown in Fig. 5, Fig. 8b and Fig. 9b are subject to the ability of the physical process to be operated in such a fashion.

The recommendations are also subject to our surface chemistry model being a reasonable representation of the process chemistry. The details of the coverage and monolayers deposited per cycle, as well as the potential for desorption during purges, depend on the chemistry model used. Though the model we use does allow fairly good fits to the available data, this does not mean we have a good chemistry model. The available data are limited and very smooth, and we expect that other models would also provide good fits. The model used is a simple model that provides reasonable fits to the data. The goal of the paper is to establish a methodology. It is clear that more reliable suggestions can be obtained, if more relevant data are presented in reports on ALD process studies.

ACKNOWLEDGMENTS

The RPI authors acknowledge support from MARCO, DARPA, and NYSTAR for the Interconnect Focus Center.

REFERENCES

- [1] M. Ritala and M. Leskela, *Nanotechnology* **10**, 19 (1999).
- [2] M. Leskela and M. Ritala, *J. Phys. IV, Colloq. C5* **5**, 937 (1995).
- [3] T. Suntola, *Thin Solid Films* **216**, 84 (1992).
- [4] H. Siimon and J. Aarik, *J. Phys. D: Appl. Phys.* **30**, 1725 (1997).
- [5] J.-W. Lim, H.-S. Park, and S.-W. Kang, *J. Electrochem. Soc.* **148** (6), C403 (2000).
- [6] H.-S. Park, J.-S. Min, J.-W. Lim, and S.-W. Kang, *Applied Surface Science* **158**, 81 (2000).
- [7] T. S. Cale, T. P. Merchant, L. J. Borucki, and A. H. Labun, *Thin Solid Films* **365**, 152 (2000).
- [8] EVOLVE is an extensible topography simulation framework. EVOLVE 5.0i was released in June 1999. © 1991-2002, T. S. Cale.
- [9] M. K. Gobbert and T. S. Cale, in *Fundamental Gas-Phase and Surface Chemistry of Vapor-Phase Deposition II*, M. T. Swihart, M. D. Allendorf, and M. Meyyappan, eds. The Electrochemical Society Proceedings Series, Vol. 2001-13, 2001, pp. 316-323.
- [10] M. K. Gobbert, S. G. Webster, and T. S. Cale, *J. Electrochem. Soc.* **149**(8), G461 (2002).
- [11] M. K. Gobbert, V. Prasad, and T. S. Cale, *Thin Solid Films* **410**(1-2), 129 (2002).
- [12] M. K. Gobbert, V. Prasad, and T. S. Cale, *J. Vac. Sci. Technol. B* **20**(3), 1031 (2002).
- [13] S. M. Rossnagel, A. Sherman, and F. Turner, *J. Vac. Sci. Technol. B* **18**(4), 2016 (2000).
- [14] J.-S. Park, M.-J. Lee, C.-S. Lee, and S.-W. Kang, *Electrochem. Solid-State Lett.* **4**(4), C17 (2001).
- [15] J.-S. Park, H.-S. Park, and S.-W. Kang, *J. Electrochem. Soc.* **149**(1), C28 (2002).
- [16] H. Kim and S. M. Rossnagel, "Growth Kinetics and Initial Stage Growth during Plasma-enhanced Ti Atomic Layer Deposition", *J. Vac. Sci. Technol. A* **20**(3), 802-808 (2002).
- [17] J. W. Klaus, S. J. Ferro, and S. M. George, "Atomic Layer Deposition of Tungsten Nitride Films using Sequential Surface Reactions", *J. Electrochem. Soc.* **147**(3), 1175-1181 (2000).